Mobility and Energy Aware Data Routing for UAV-Assisted VANETs

Hakim Ghazzai[1], Ahmed Khattab[2], and Yehia Massoud[1]
[1]School of Systems and Enterprises – Stevens Institute of Technology, Hoboken, NJ, USA
e-mail: {hghazzai, ymassoud}@stevens.edu
[2]Electronics and Electrical Communications Engineering Department – Cairo University, Giza, Egypt
e-mail: akhattab@ieee.org

***Abstract*—In this paper, we develop a mobility and energy aware data routing protocol for unmanned aerial vehicle-assisted vehicular ad-hoc networks (UAV-assisted VANETs). One of the UAV act as a flying roadside Uunit (RSU) collecting data from ground vehicles, while the other UAVs play the role of relays to deliver the data to mobility service center (MSC). The UAVs can adjust their three-dimensional (3D) locations within a predefined range, if needed, in order to ensure reliable communication links. The proposed approach aims to minimize the energy consumed by the UAVs in both data transfer and movement. which ensures fair distribution of the routing effort across the different UAVs in the network. This is achieved by taking the residual UAV energy into account in the routing decision. We formulate such a routing problem as a mixed integer non-linear program (MINLP) to determine both the selected route and the locations of the UAVs participating in the data transfer process. Since such a problem is non-convex, we proceed with a joint optimization solution where the route is optimized using an ILP and the UAVs' 3D locations are determined using the meta-heuristic particle swarm optimization (PSO) algorithm. We present a selected set of numerical results to illustrate the performance of the proposed solution for different scenarios and compare it to a meta-heuristic approach based on swarm intelligence.**

***Index Terms*—Data routing, flying RSU, vehicular ad-hoc networks, unmanned aerial vehicle.**

I. INTRODUCTION

Intelligent transportation systems (ITSs) are major building blocks of contemporary smart cities. Even though it has recently witnessed significant development and deployment, such a technology is continuing to evolve. For instance, currently, the information and communication technologies (ICT) infrastructure deployed in ITSs relies on roadside units (RSUs) statically installed on the sides of the roads. Vehicles are equipped with dedicated short range communications (DSRC) interfaces that allow for the data transfer between the vehicles amongst themselves and with the RSUs. The RSUs in turn relays the vehicles' data to a remote mobility service center (MSC) for further processing. The recently emerging unmanned aerial vehicles (UAVs), a.k.a. drones, are currently investigated as an enabling technology for flying RSUs [1]. With these low-cost multi-rotor UAVs, better communication links can be established thanks to their mobility at high altitude, which allows for higher probability to establish line-of-sight (LoS) communication links with ground vehicles. Moreover, their mobility allows for better flexibility in covering traffic events especially during emergency situations. However, UAVs suffer from a limited battery issue, which handicaps their missions and restrains their operations to short-term periods.

Even though they have been used in military for several years, UAVs have been recently used in multitude of civilian applications. Examples include the delivery of merchandize and services, security and surveillance, and precision agriculture [2]. In ITS, UAVs can be used to perform traffic management tasks and report possible traffic violations [3]. UAVs flying in the vicinity of an accident can be used to provide basic support or report the situation especially if equipped with cameras. UAVs can also play the role of a flying traffic police officer [2]. Alternatively, UAVs can also be used as flying RSUs that collect data to/from the vehicles and route it from/to remote destinations such as the mobility service center. The use of UAVs for such vehicular data collection and dissemination tasks results in what is known for UAV-assisted vehicular ad-hoc network (UAV-assisted VANET).

In this paper, we present a multi-objective routing protocol which aims to minimize a weighted average of the different energies consumed by the UAVs and well as the residual energy amiable at the UAVs. Our approach increases the overall UAV network lifetime and ensures fairness in the energy consumption of the different UAVs. More specifically, we consider a UAV-assisted VANET in which some of the flying RSUs are selected to transfer the data from a vehicle (acting as the data source) to a remote basestation (action as a destination). Some UAVs are allowed to slightly change their locations when the communication link is not good in order to ensure reliable transmission. We formulate such a multi-objective routing problem as a mixed integer nonlinear programming (MILP) problem and solve it using a joint exploratory search algorithm, which, alternately, searches for the data route and the three-dimensional (3D) locations of the UAVs. On the one hand, an ILP is executed to find a data route given fixed UAVs' locations. On the other hand, a meta-heuristic particle swarm optimization (PSO) is implemented to determine the best 3D locations of the flying relays. The developed routing algorithm finds the best directions and distances according to which the UAVs will move within a pre-defined range to establish seamless links for data routing. Selected simulation results investigate the performance of the proposed approach for different metric combinations and show

how the UAVs behave with respect to the ground vehicle need.

II. Related Work

The UAV-assisted VANET literature mainly investigates the placement and path planning problems for UAVs [4], [5]. The main objectives are to achieve better connectivity and ensure reliable data transfer. Only few works have addressed the data routing problem in UAV-assisted VANETs [6]–[9]. For instance, two data routing approaches based on optimized link-state routing (OLSR) protocol were proposed and experimentally evaluated in [6]. The performance of both algorithms was assessed in networks with frequent topology changes. Meanwhile, the authors of [7] avoided connectivity loss between ground vehicles by having the flying UAVs autonomously positioning themselves to act as relays between the vehicles. The proposed approach is based on using the Hello messages. Alternatively, a combined omnidirectional/directional transmission scheme, with dynamic angle adjustment capability, was proposed in [8]. The objective of such a scheme was to use the location and trajectory information for performing unicast and geocast routing. In order to enhance the routing protocol's efficiency, prediction mechanisms were used to determine the UAV's location and its trajectory. Finally, the authors of [9] developed a routing algorithm that allows the flying UAVs to change their location within a certain range to minimize the packet transmission time and ensure a reliable communication. However, the focus was to only minimize the packet transmission time without regard to other factors such as the available energy at the UAVs and the energy consumed in communication or movement.

III. System Model

We consider a VANET operating in an urban area in which vehicles use the DSRC protocol to communicate with each other and with the RSUs. Unlike traditional studies which typically employ static RSUs installed on the road sides, we consider flying RSUs. Flying RSUs are UAVs equipped with DSRC interfaces, which can either communicate directly with ground vehicles or with each other to forward the data to MSC, as shown in Fig. 1. Let N denotes the number of UAVs used to cover the area of interest. The initial locations of the UAVs are predefined by the ITS operator at the geographical coordinates $X_n^0 = (x_n^0, y_n^0, z_n^0)$, where $n \in \mathcal{N} = \{1, \ldots, N\}$, in a 3D space. Once an event, e.g., accident, occurs, a vehicle generates a packet of length M and transmits it to the flying RSU network using DSRC technology. The message will be then routed through the flying RSU network to reach a remote basestation or access point that serves as gateway to the MSC that handles the message. Let the coordinates of the colliding vehicle, i.e. the source node, be located at $X_s^0 = (x_s^0, y_s^0, z_s^0)$. The coordinates of the basestation destination are $X_d^0 = (x_d^0, y_d^0, z_d^0)$.

A. Channel Model

In the considered system model, there are two different channel models. The first one is for the links between a UAV and a ground node (either a vehicle or a basestation). The second model is for the communication channels amongst the UAVs.

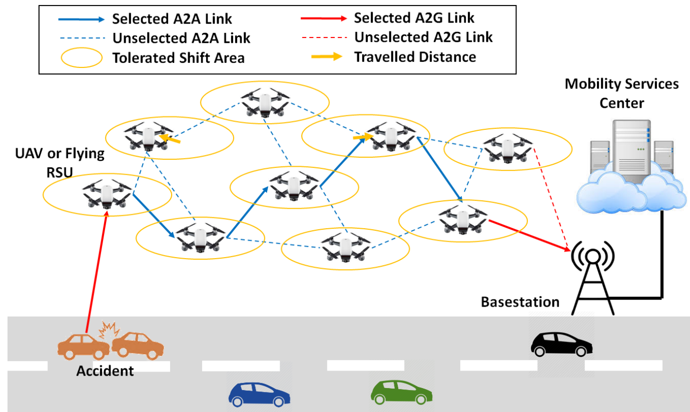

Fig. 1: UAV-assisted vehicular network architecture where UAVs act as either a flying RSU communication with a ground vehicle or a flying relay forwarding data to MSC.

1) Air-to-Ground Channel Model: A vehicle or a basestation may have a LoS link to the flying RSU communicating with. Alternatively, obstacles might exist between the node on the ground and the UAV resulting in a partial non-LoS (NLoS) effect. Having a LoS or NLoS link depends on the UAV's altitude z_n: the higher the UAV's altitude the higher the chance of having a LoS link. It was shown in [10] that the probability that a ground node, denoted by $m \in \{s, d\}$ and a UAV n have a LoS link given by:

$$P_r = \frac{1}{1 + B\exp(-C[\theta(h_n, d_{nm}) - B])}, \tag{1}$$

where the constants B and C are dependent on the environment and $\theta = \frac{180}{\pi}\sin^{-1}(\frac{z_n}{d_{nm}})$ represents the elevation angle that depends on the distance separating the two nodes d_{nm}. Hence, the air-to-ground (A2G) path loss (in dB) is given by:

$$PL^{\text{A2G}}[\text{dB}] = P_r\, PL^{\text{LoS}} + (1 - P_r)\, PL^{\text{NLoS}}, \tag{2}$$

where PL^{LoS} and PL^{NLoS} are the LoS and NLoS path losses (expressed in dB), respectively.

We adopt the measurement-driven model of DSRC communication in ITS applications presented in [11] to compute the LoS and NLoS path losses. The model of [11] follows the log-distance power law. Accordingly, the path loss is expressed as:

$$PL^{\text{X}}(d_{nm}) = PL_0^{\text{X}} + 10\gamma^{\text{X}} \log_{10} d_{nm} + S^{\text{X}}, d_{min} \leq d \leq d_{max}, \tag{3}$$

where $\text{X} \in \{\text{LoS}, \text{NLoS}\}$ to indicate a LoS or NLoS path loss, PL_0^{X} is a path loss constant that relates to the reference distance, γ^{X} is the environment path loss exponent, and d_{min} and d_{max} are the bounds on the distance within which the model is valid. Such bounds were driven from measurement campaigns [11]. To model the large-scale fading of the environment, a zero-mean random normal distribution with standard deviation σ_S^{X}, denoted by S^{X}, is used.

2) Air-to-Air Channel Model: The air-to-air (A2A) channel model describes the link between the different UAVs. Due to the lack of obstacles, A2A links are dominated by a free-space

LoS propagation. The A2A LoS path loss (in dB) between two UAVs n and m is given as [12]:

$$PL_{nm}^{\text{A2A}}[\text{dB}] = 10\eta \log_{10}\left(\frac{4\pi f d_{nm}}{C_l}\right) + L^{\text{LoS}}, \quad (4)$$

where η is the free-space path loss exponent, f is the DSRC carrier frequency, d_{nm} is the distance between the n^{th} and the m^{th} UAVs, C_l is the speed of the light, and L^{LoS} is an attenuation term that is added to the LoS environment.

It is worth noting that, for both the A2G and A2A channel models, the small scale fading impact is negligible. This is because we assume that some of the UAVs slightly move from their original locations. This results in a flying time that is usually much larger than the coherence time of the channels. Hence, our work relies on the average statistics of the channel.

B. UAV Energy Model

The energy consumed by the n^{th} UAV to perform a complete data transfer is composed of two components: a motion energy that is consumed due to the movement of the UAV to adjust its location for data transfer and a communication energy component that is used for the data transfer from the n^{th} UAV to another node.

To compute the motion energy, we adopt the following accurate mobility power model, presented in [13], that depends on different parameters including the speed of the UAV V_n:

$$P_n^M = P_0\left(1 + \frac{3{V_n}^2}{U_{tip}^2}\right) + P_i\left(\sqrt{1 + \frac{{V_n}^4}{4v_0^4}} - \frac{{V_n}^2}{2v_0^2}\right)^{\frac{1}{2}} + \frac{1}{2}d_0\rho s A{V_n}^3, \quad (5)$$

where P_0 and P_i are two power constants representing the blade profile and the induced power levels in hovering status, respectively, U_{tip} denotes the tip speed of the rotor blade, v_0 is known as the mean rotor induced velocity in hover, d_0 and s are the fuselage drag ratio and rotor solidity, respectively, and ρ and A denote the air density and rotor disc area, respectively. When stationary hovering, the speed V_n is set to zero and hence, the hovering power is equal to $P_{\text{hov}} = P_0 + P_i$. The mobility energy is then expressed as follows:

$$E_n^M = P_n^M T_n^f, \quad (6)$$

where T_n^f denotes the flying time of the UAV n when it adjusts its position from its initial location an initial location X_n^0 to another location X_n^f. We denote the corresponding traveled distance by Δ_n. Hence, the flying time $T_n^f = \frac{D_n}{V_n}$. It should be noted that UAVs can adjust their locations only within a predefined region: a circle centered at their initial locations with a radius $\bar{\Delta}$.

When transmitting data, the UAV n will stationary hover and then transmit data to another node (another UAV or the basestation). Hence, we propose that the communication energy of UAV n is expressed as the sum of the communication energy and the hovering energy when receiving the message from a node $m' \in \{s, \mathcal{N}\}$ and retransmitting it to another node $m \in \{\mathcal{N}, d\}$ as follows:

$$E_n^C(m', m) = \epsilon_{m'n} P_{\text{hov}} T_{m'}^C(n) + \epsilon_{nm}\left(P_{\text{hov}} + P_n^C\right) T_n^C(m), \quad (7a)$$

$$\text{where } P_n^C = \mu P_n + \nu, \quad (7b)$$

where P_n^C is the communication interface power of UAV n that is approximately linearly related to UAV's transmit power level P_n as given in [14]. The scaling parameter μ adjusts the radiated power and the constant power ν models the hardware circuit processing power. The binary variable ϵ_{nm} equals 1 if the link between n and m is used for transmission and 0 otherwise. Finally, $T_n^c(m)$ denotes the time needed to transfer the message from the n^{th} UAV to another node m. The communication time over the link between the n^{th} UAV and the m^{th} node is inversely proportional to the corresponding achievable rate, $R_n(m)$, which is in turn affected by the path loss effect as follows:

$$T_n^C(m) = \frac{M}{R_n(m)}. \quad (8)$$

To compute the data rate, we adopt a truncated Shannon expression as follows:

$$R_n(m) = \begin{cases} R_{\max}, & \text{if } \text{SINR}_n(m) \geq \text{SINR}_{\max}, \\ 0, & \text{if } \text{SINR}_n(m) \leq \text{SINR}_{\min}, \\ W\log_2\left(1 + \text{SINR}_n(m)\right), & \text{otherwise}, \end{cases} \quad (9)$$

where $R_{\max}$ is given by $R_{\max} = W\log_2(1 + \text{SINR}_{\max})$. The parameter W corresponds to the DSRC protocol bandwidth, while $\text{SINR}_n(m)$ denotes the signal-to-interference-plus-noise ratio (SINR) of the link between n and m. The $\text{SINR}_n(m)$ is expressed as given below:

$$\text{SINR}_n(m) = \frac{P_n H_n(m)}{I + N_0}, \quad (10)$$

where $H_n(m)$ is the corresponding channel power of the link between m and n and is equal to $H_n(m) = \frac{1}{PL_{nm}^{\text{X}}}$ where $\text{X} \in \{\text{A2G}, \text{A2A}\}$, I is the average interference power, and N_0 is the additive noise power. Finally, $\text{SINR}_{\min}$ and $\text{SINR}_{\max}$ are the SINR thresholds for the discretization of the data rate in DSRC technology.

Note that, in this paper, we are interested in the UAV energy only since it is the most critical one. The basestation and the ground vehicle energy are out of the scope of this paper.

IV. UAV-based Routing Problem Formulation

In this paper, we formulate an optimization problem that finds the best route in the UAV-assisted VANET composed of the N flying units to forward the data packet generated by a source vehicle to the destination basestation. The criterion of selecting the path in this work is based on minimizing a multi-objective cost function the reflects the different energies consumed by the UAVs for the transmission of a message of size M as well as their residual energies. Hence, the utility metric $\mathcal{U}$ corresponds to a weighted sum of these three energy metrics and is expressed as follows:

$$\mathcal{U} = \sum_{n=1}^{N} \pi_n \left(\omega_1\left(1 - \frac{E_n^R}{\bar{E}^R}\right) + \omega_2 \frac{E_n^C}{\bar{E}^C} + \omega_3 \frac{E_n^M}{\bar{E}^M}\right), \quad (11)$$

where the denominators' parameters $\bar{E}^R$, $\bar{E}^C$, and $\bar{E}^M$ are used to normalize the metrics such that their values will be between zero and one. For instance, $\bar{E}^R$ can be the maximum battery capacity of all UAVs and $\bar{E}^C$ and $\bar{E}^M$ are the maximum possible communication and motion energy levels, respectively. In (11), ω_i with $i \in \{1, 2, 3\}$ denotes the weights associated to each energy objective. Their values $\in [0, 1]$ are chosen by the ITS operator. Finally, π_n is an endogenous binary variable indicating whether the UAV n is participating to the data transfer or not. It is equal 1 if it is the case. It can be expressed as a function of ϵ_{mn} as follows:

$$\pi_n = \sum_{m \in \{s, \mathcal{N}\}} \epsilon_{nm}, \forall n \in \{\mathcal{N}, d\}. \tag{12}$$

It is worth to note that the value of the residual energy is E_n^R is known before the data routing procedure and is updated every time the transmission is completed, while the values of the communication and motion energies E_n^C and E_n^M depend on two decision variables: the link selection binary variable ϵ_{nm} and the continuous UAV location variable X_n^f. The optimization problem for data routing with relay positions adjustment for UAV-assisted VANET can be, then, formulated as follows:

$$\underset{\substack{\epsilon_{nm} \in \{0,1\}, X_n^f \in \mathbb{R}+ \\ \forall m \in \{s, \mathcal{N}\}, \forall n \in \{\mathcal{N}, d\}}}{\text{minimize}} \quad \mathcal{U} \tag{13a}$$

subject to

$$\sum_{m \in \mathcal{N}} \epsilon_{mn} - \sum_{m \in \mathcal{N}} \epsilon_{nm} = \begin{cases} 1, & \text{if } n = d, \\ 0, & \text{if } n \in \mathcal{N}, \\ -1, & \text{if } n = s, \end{cases} \tag{13b}$$

$$\sum_{m \in \mathcal{N}} \epsilon_{nm} \le 1, \quad \forall n \in \mathcal{N}, \tag{13c}$$

$$\epsilon_{nm} + \epsilon_{mn} \le 1, \quad \forall n, m \in \mathcal{N}, \tag{13d}$$

$$\epsilon_{nm} \le \delta_{nm}, \quad \forall n, m \in \mathcal{N}, \tag{13e}$$

$$E_n^C + E_n^M \le \bar{E}_n, \quad \forall n \in \mathcal{N}, \tag{13f}$$

$$\Delta_n(X_n^0, X_n^f) \le \pi_n \bar{\Delta}, \quad \forall n \in \mathcal{N}. \tag{13g}$$

Below, we define the different constraints of the UAV-based data routing problem:

- Constraints (13b) ensure a smooth data flow conservation in the network and guarantees that the data sent from the source reaches the destination,
- Constraint (13c) imposes that a UAV can transmit the data to at maximum one UAV,
- Constraint (13d) the flying network avoids the cyclic transmission within a single link. Together, constraints (13b)-(13d) are set in order to avoid cyclic data routing such that a UAV will receive the message only once during the routing.
- Constraint (13e) indicates that the data transfer can only be possible over seamless links, i.e, $\delta_{nm} = 1$ when $R_{nm} > 0$ according to (9).
- Constraint (13f) indicates that the total energy consumed by the UAV during the position adjustment, the data transmission, and data reception has to be less than the available energy in its battery.
- Finally, constraint (13g) indicates that, when adjusting its position, a UAV cannot be shifted with a distance higher than $\bar{\Delta}$.

The optimization problem formulated in (13) is categorized as a MINLP whose optimal solution is difficult to obtain. Therefore, in the next section, we propose a joint iterative algorithm alternating between the determination of the data route ϵ_{nm} and the 3D locations of the UAVs X_n^f.

V. Proposed Joint Iterative Algorithm

In this section, we devleop the proposed joint iterative algorithm where the 3D locations of the UAVs are optimized using the meta-heuristic algorithm. At each iteration of the PSO, the positions are fixed and an ILP is executed to determine the corresponding data routing path minimizing the metric $\mathcal{U}$. This process is repeated till the PSO converges. We start by discussing the ILP and then, present the full algorithm.

A. Integer Linear Program for Data Routing

In this step, we assume fixed 3D UAV positions, e.g., selected randomly within the pre-defined range or can be the initial locations. In this case, the optimization problem (13) is converted to an ILP with respect to the variable ϵ_{nm} only. Solving the ILP can be optimally performed using the branch and bound algorithm implemented in off the shelf software such as CPLEX or CVX. It may happen that some of the links are not seamless $\text{SINR} \le \text{SINR}_{\min}$ which may prevent the ILP to find a feasible solution given the current locations of the UAVs. To avoid such a scenario, we propose to relax the problem and set $\text{SINR}_{\min}$ as follows $\text{SINR}_{\min} = M$ dB where M is a very low SINR value such that feasible solutions are guaranteed although it is not realistic. We proceed with this relaxation assumption in order to allow the PSO determines whether it is exploring correct search directions. Once the PSO, described in Section V-B, converges, the $\text{SINR}_{\min}$ is reset to each original value and the ILP is re-executed to verify whether the final solution is feasible or not. Indeed, given the limited pre-defined regions within which the UAVs can move or for insufficient available energy, routing cannot be possible even after adjusting the relay positions.

B. Particle Swarm Optimization for UAV Positionning

The reason behind using the meta-heuristic algorithm PSO is its effective ability to achieve near optimal solutions for many engineering problems [15]. Compared to other evolutionary and meta-heuristic approaches, PSO proceeds with a simple search process, which makes its implementation easy by manipulating few parameters such as the number of particles and acceleration factors. In addition, it does not demand high computational resources to converge.

We denote by $\boldsymbol{X}$ the $N \times 3$ matrix containing the different 3D locations of the N UAVs. To optimize the matrix $\boldsymbol{X}$, PSO forms an initial generation by randomly generating P particles $\{\boldsymbol{X}_{g=0}(p),\ p = 1, \cdots, P\}$ (Line 3). Then, for each particle p, in other words, for each UAV locations combination, it solves the ILP described in Section V-A to determine the corresponding data route $\epsilon_{mn}(p)$ and evaluate the associated product $\text{SINR}_{\min} \times \mathcal{U}(p)$ (Line 6). Next, after recording the

Algorithm 1 Joint PSO-ILP algorithm for data routing in UAV-assisted VANET

1: Set $g \leftarrow 0$.
2: Set $\text{SINR}_{\min} \leftarrow M$.
3: Generate an initial generation g composed of P random particles $\boldsymbol{X}_g(p)$.
4: **while** Not converged **do**
5:     **for** $p := 1, \cdots, P$ **do**
6:         Solve the ILP problem given in (13) given the locations in $\boldsymbol{X}_g(p)$.
7:         Compute the corresponding utility metric $\text{SINR}_{\min} \times \mathcal{U}_g(p)$.
8:     **end for**
9:     Find the global particle $\boldsymbol{X}^{\text{G}}$ and the local position $\boldsymbol{X}^{\text{L}}(p)$ for each particle p.
10:     Adjust the velocities and positions of all particles using equations (14) and (15).
11:     **if** $\boldsymbol{X}^{\text{G}}$ is updated **then**
12:         $M \leftarrow M + \delta_M$.
13:     **end if**
14:     $g \leftarrow g + 1$.
15: **end while**
16: Re-set $\text{SINR}_{\min}$.
17: Solve the ILP problem given in (13) given the locations in $\boldsymbol{X}^{\text{G}}$.

result of each particle, PSO identifies the global particle that provides the highest utility value, denoted by $\boldsymbol{X}^{\text{G}}$. In addition, for each particle n, it maintains a record of the position corresponding to its best performance known as the local position and denoted by $\boldsymbol{X}^{\text{L}}(p)$ (Line 9). Then, PSO computes a velocity term $\boldsymbol{V}_g(p)$ as follows:

$$\boldsymbol{V}_g(p) = \xi \boldsymbol{V}_{g-1}(p) + r_{1g}\left(\boldsymbol{X}^{\text{L}}(p) - \boldsymbol{Z}_g(p)\right) + r_{2g}\left(\boldsymbol{X}^{\text{G}} - \boldsymbol{X}_g(p)\right), \quad (14)$$

where ξ is the inertia weight and r_{1g} and r_{2g} are two elements uniformly generated $\in [0, 2]$ for each generation g [15]. Then, PSO updates each particle $\boldsymbol{X}_g(p)$ as follows:

$$\boldsymbol{X}_g(p) = \left[\boldsymbol{X}_g(p) + \boldsymbol{V}_g(p)\right]_{\boldsymbol{C}}, \quad (15)$$

where $[.]_{\boldsymbol{C}}$ ensures that the new obtained UAV position are within the circle with radius $\bar{\Delta}$ and centered at X_n^0 for each UAV n.

If the global value is updated, then we proceed by increasing the value of $\text{SINR}_{\min}$ to allow PSO looks for more realistic solutions. The PSO's particles are updated till convergence is reached, i.e., when the utility function is no more improving after a certain number of iterations or when the maximum number of iterations is attained. The joint ILP-PSO algorithm is presented in Algorithm 1.

VI. Performance Evaluation

In this section, we present some selected results to investigate the behavior of the proposed joint optimization algorithm. The simulations are executed in an area of size $1500 \times 600 \times 60$ m^3. The altitudes of the UAVs are randomly chosen between 20 and 60 meters. The UAVs cannot move more than $\bar{\Delta} = 400$ meters in all directions. The batteries' capacities of the UAVs are linearly decreasing according to their indexes as follows $\bar{E}_n = \bar{E}_1 - n\frac{\bar{E}_1}{N}$, where $\bar{E}_1 = 83$ Wh. We perform this choice in order to visualize the data routing when considering the

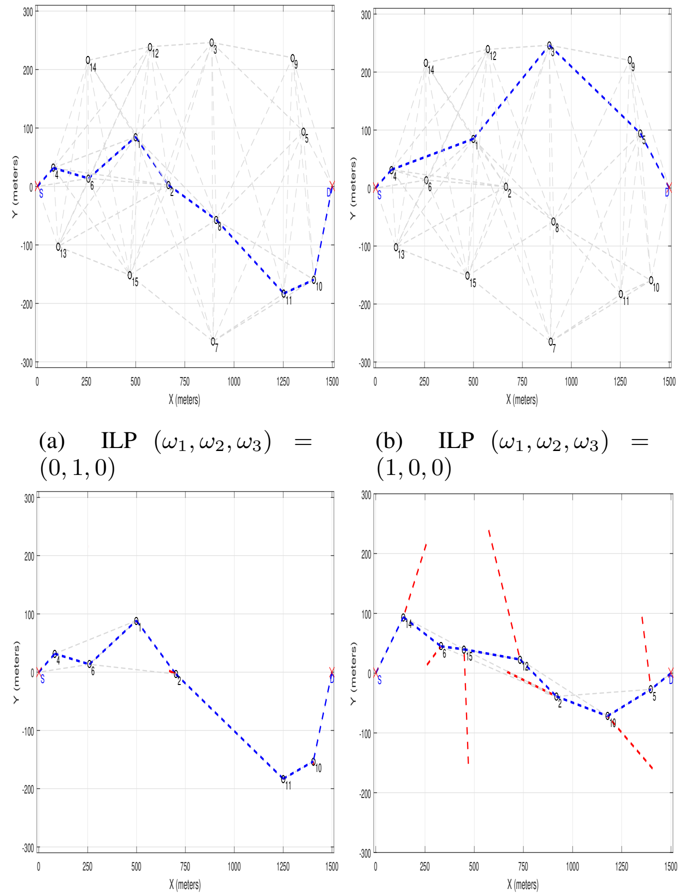

(a) ILP $(\omega_1, \omega_2, \omega_3) = (0, 1, 0)$

(b) ILP $(\omega_1, \omega_2, \omega_3) = (1, 0, 0)$

(c) Joint ILP-PSO $(\omega_1, \omega_2, \omega_3) = (0, \frac{1}{2}, \frac{1}{2})$.

(d) Joint ILP-PSO $(\omega_1, \omega_2, \omega_3) = (0, 1, 0)$.

Fig. 2: Four data routing scenarios using the proposed algorithm (black circles: UAVs, Red crosses: source and destination, blue dashed lines: data route, gray dashed lines: potential communication link, and red dashed lines: UAV mobility).

residual energy metric only. The source and the destination are placed at the locations $(0, 0, 1)$ and $(1500, 0, 1)$, respectively, and aim to exchange a message of size $M = 3200$ octets. The frequency carrier of the DSRC protocol is chosen to be $f = 5.9$ GHz and, as parameters of the DSRC channels for the LoS and NLoS links, we select the mean values of the urban (high density) scenario with a bandwidth $W = 10$ Mhz [11]. We set $\text{SINR}_{\min} = -6.37$ dB and $\text{SINR}_{\max} = 7.35$ dB. The UAV mobility power model are obtained from [13]. The UAV communication power parameters are set as follows: $\mu = 2.4$, $P_n = 23$ dBm, $\forall n \in \{s, \mathcal{N}, d\}$, and $\nu = 5$ W. The PSO is executed for at maximum 200 iterations and $P = 8$ particles.

In Fig 2, we present four data routing scenarios with $N = 15$ UAVs randomly located in the area of interest. In Fig 2a and Fig 2b, we provide the cases where all the UAVs are able to participate for the data routing and hence, ILP-based solution is provided since mobility is not required to route the data. The figures plot the data routes while only minimizing (a) the communication energy (i.e., $\omega_1 = 0$, $\omega_2 = 1$, and $\omega_3 = 0$ in Fig 2a) and (b) the residual energy metric (i.e., $\omega_1 = 1$, $\omega_2 = 0$, and $\omega_3 = 0$ in Fig 2b). We can notice, for the first

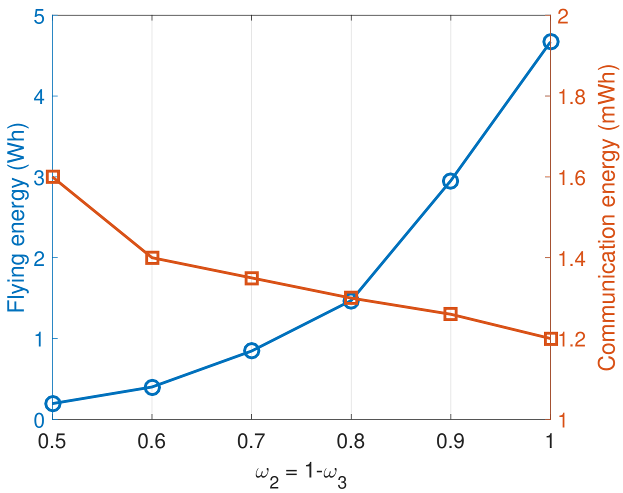

Fig. 3: Communication energy versus flying energy for different weights ($\omega_1 = 0$ and $\omega_2 = 1 - \omega_3$).

scenario, the ILP chooses the fastest route with highest channel quality where the UAVs are close to each other, while, for the second scenario, the ILP selects the UAVs with low indexes as they posses higher residual energy levels. In both previous cases, motion energy is zero since the UAVs are stationary hovering when forwarding the data.

In Figs. 2c and 2d, we visualize the scenarios where some of the UAVs adjust their locations in order to find 3D locations at which they can support the ground nodes. To do so, we force $\bar{E}_3 = \bar{E}_7 = \bar{E}_8 = 0$ Wh, which divides the network into two left and right clusters. In Fig. 2c, we provide the obtained solution using the joint ILP-PSO algorithm for the case where communication energy only matters for the ITS operator. For clarity, we plot only the UAVs participating to the data routing. We can notice that in order to establish a seamless link with UAV 11, UAV 2 has shifted its location in the direction of the right cluster by around 44 meters. Finally, in Fig.2c, we choose the same weight combination as in Fig 2a. We notice here that the UAVs enjoy complete freedom to move and have a unique objective: the minimization of the communication energy, which is equivalent to the maximization of the overall links' data rates.

In Fig. 3, we vary the weights of the consumed communication and flying energy as follows $\omega_2 = 1 - \omega_3$ while setting $\omega_1 = 0$. We can clearly see that when the $\omega_2 \rightarrow 1$, the consumed energy is minimized to around 1.2 mWh while the flying energy is maximized to around 3 Wh. Hence, in this regime, the optimizer will move the UAVs such that maximum data rate is obtained. In the opposite case, when $\omega_2 \rightarrow 0.5$ (Due to the different magnitude levels, the minimum weight is 0.5. Values lower than 0.5 provide similar results), the flying energy is minimized where minor position adjustments are made to ensure minimum data rate (i.e., SINR $\geq$ SINR$_{\min}$) so data can be forwarded to destination. Other values of ω_2 achieves a tradeoff between both energy levels, in other words, mobility versus data throughput.

VII. Conclusion

In this paper, we have developed a mobility and energy aware joint optimization algorithm for data routing in UAV-assisted VANETs. The UAVs acting as flying RSUs and relays intercept data from ground vehicles and forward it to the MSC. Whenever communication links are absent, the UAV topology is modified given energy and mobility constraints such that seamless data transfer can be established. Three energy metrics, namely residual, communication, and flying energies are simultaneously minimized according to the associated weight. A MINLP problem is formulated and solved using an iterative algorithm alternating between ILP and PSO to jointly determine the data route and the UAVs' locations. As a future work, we will focus on designing a decentralized approach where UAVs will decide both their locations and to which node forward the data.

References

[1] H. Menouar, I. Guvenç, K. Akkaya, A. S. Uluagac, A. Kadri, and A. Tuncer, "UAV-enabled intelligent transportation systems for the smart city: Applications and challenges," *IEEE Communications Magazine*, vol. 55, no. 3, pp. 22–28, Mar. 2017.

[2] I. Bekmezci, O. K. Sahingoz, and S. Temel, "Flying ad-hoc networks (fanets): A survey," *Ad Hoc Networks*, vol. 11, no. 3, pp. 1254 – 1270, 2013. [Online]. Available: http://www.sciencedirect.com/science/article/pii/S1570870512002193

[3] H. Ghazzai, H. Menouar, A. Kadri, and Y. Massoud, "Future uav-based its: A comprehensive scheduling framework," *IEEE Access*, vol. 7, pp. 75 678–75 695, June 2019.

[4] Z. Han, A. L. Swindlehurst, and K. J. R. Liu, "Optimization of MANET connectivity via smart deployment/movement of unmanned air vehicles," *IEEE Trans. Veh. Technol.*, vol. 58, no. 7, pp. 3533–3546, Sept. 2009.

[5] G. J. Lim, S. Kim, J. Cho, Y. Gong, and A. Khodaei, "Multi-UAV pre-positioning and routing for power network damage assessment," *IEEE Transactions on Smart Grid*, vol. 9, no. 4, pp. 3643–3651, July 2018.

[6] S. Rosati, K. Krużelecki, G. Heitz, D. Floreano, and B. Rimoldi, "Dynamic routing for flying ad hoc networks," *IEEE Trans. Veh. Technol.*, vol. 65, no. 3, pp. 1690–1700, Mar. 2016.

[7] O. S. Oubbati, A. Lakas, N. Lagraa, and M. B. Yagoubi, "UVAR: An intersection UAV-assisted VANET routing protocol," in *IEEE Wireless Communications and Networking Conference (WCNC 2016)*, Doha, Qatar, Apr. 2016.

[8] G. Gankhuyag, A. P. Shrestha, and S. J. Yoo, "Robust and reliable predictive routing strategy for flying ad-hoc networks," *IEEE Access*, vol. 5, pp. 643–654, Jan. 2017.

[9] H. Ghazzai, A. Feidi, H. Menouar, and M. L. Ammari, "An exploratory search strategy for data routing in flying ad hoc networks," in *IEEE Annual International Symposium on Personal, Indoor, and Mobile Radio Communications (PIMRC'17)*, Montreal, Canada, Oct. 2017.

[10] A. Al-Hourani, S. Kandeepan, and S. Lardner, "Optimal LAP altitude for maximum coverage," *IEEE Wireless Communications Letters*, vol. 3, no. 6, pp. 569–572, Dec. 2014.

[11] H. Fernández, L. Rubio, V. M. Rodrigo-Peñarrocha, and J. Reig, "Path loss characterization for vehicular communications at 700 MHz and 5.9 GHz under LOS and NLOS conditions," *IEEE Antennas and Wireless Propagation Letters*, vol. 13, pp. 931–934, 2014.

[12] A. Al-Hourani, S. Kandeepan, and A. Jamalipour, "Modeling air-to-ground path loss for low altitude platforms in urban environments," in *IEEE Global Communications Conference (Globecom 2014)*, Austin, TX, USA, Dec. 2014.

[13] Y. Zeng, J. Xu, and R. Zhang, "Energy minimization for wireless communication with rotary-wing UAV," *IEEE Transactions on Wireless Communications*, vol. 18, no. 4, pp. 2329–2345, Apr. 2019.

[14] G. Auer et al., "Energy efficiency analysis of the reference systems, areas of improvement and target breakdown," Tech. Rep., INFSO-ICT-247733 EARTH (Energy Aware Radio and NeTwork TecHnologies), Jan. 2012.

[15] M. Clerc and J. Kennedy, "The particle swarm-explosion, stability, and convergence in a multidimensional complex space," *IEEE Transactions on Evolutionary Computation*, vol. 6, no. 3, pp. 58–73, Feb. 2002.